

## 科技部補助

### 大專學生研究計畫研究成果報告

\* \*\*\*\*\* \*\*\*\*\* \*  
\* 計畫 The role of potassium channels in regenerating \*  
\* : axonal conduction following end to end \*  
\* 名稱 neurorrhaphy. \*  
\* \*\*\*\*\* \*\*\*\*\* \*

執行計畫學生： 吳宗桓

學生計畫編號： MOST 103-2815-C-040-039-B

研究期間： 103年07月01日至104年02月28日止，計8個月

指導教授： 廖玟潔

處理方式： 本計畫涉及專利或其他智慧財產權，2年後可公開查詢

執行單位： 中山醫學大學醫學系解剖學科

中華民國

104年03月29日

## **Abstract**

Owing to traffic accident, trauma, and industrial injuries, peripheral nerve injury (PNI) is common in our recent society. It has been known that voltage-gated potassium channels (Kv channels) regulate the excitability of nerve and play a critical role in axonal conduction. Among the diverse family of Kv channels, Kv1.1 channels are responsible for limiting the re-excitation of the node of Ranvier and maintaining a stable nodal resting potential.

Following disruption of the myelin there is an increased activity of these channels which suppresses the membrane potential close to the equilibrium potential of  $K^+$  and results in axonal conduction blockade. However, the relationship between Kv1.1 channels localization and distribution of potassium ion on the regenerating process remains largely underexplored. To address these questions, we focus on getting to know how expression of Kv1.1 channel rearrange and mediate efflux of potassium ion following end-to-end neurorrhaphy (EEN) in rats.

EEN was performed microscopically. The specific localization of Kv1.1 channel as well as its correlation with the regenerating axons at juxtaparanodal region was examined by confocal microscopy. To perform the dynamic interaction of Kv1.1 channel and  $K^+$  in the regenerating nerve, we concentrated on potassium image at the regenerating node of Ranvier by using Time-of-Flight Secondary Ion Mass Spectrometry (TOF-SIMS). Immunofluorescence was used to examine the changes in Kv1.1 channels localization during the first three months following EEN.

Confocal photomicrographs showed that Kv1.1 channels diffusely scattered along the regenerating axons at the time 1 month following EEN, and reconstructed at the juxtaparanodal region 3 months after EEN, as it localized in normal nerve tissue. Western blot analysis revealed that the level of Kv1.1 channel for EE1M-rats and EE3M-rats were increased 1.58-fold and 1.49-fold, respectively. On the other hand, ionic image revealed that the efflux of potassium ion was decreased, and clustered at the node of Ranvier 3 months after EEN.

These results provided new information about the redistribution and expression of the Kv1.1 channels after EEN. Our findings suggest that the Kv1.1 channels reconcentrated at the juxtaparanodal regions of remyelinated axons is essential to modulate the patterns of  $K^+$  distribution on axons for maintaining stability of the membrane potential in the regenerating axons after EEN.

**Keywords:** voltage-gated potassium channels (Kv channels); Kv1.1 channel; end-to-end neurorrhaphy (EEN); remyelinated axon; juxtaparanodal region

## Introduction

With the coming of the industrialization, peripheral nerve injury (PNI) has gradually become one of the most common and important injuries in our society (Evans 2001; Priestley 2007). Peripheral nerve regeneration, conduction, and restoring muscle function after PNI is still takes a long time of approximately three months (Liao, Chen et al. 2009; Liao, Chen et al. 2010).

Axon injury is associated with demyelination, remyelination and exposure of juxtaparanodal potassium channels. In the mammalian, voltage-gated potassium channels (Kv channels), present in juxtaparanodal regions, open and close upon changes in the transmembrane potential. Kv channels are one of the key components in generation and propagation of electrical impulses in nervous system. Demyelination of intact axons by disease or injury results in altered distribution of the nodal/ paranodal ion channels and cell adhesion proteins, thus hampering the propagation of action potentials (Poliak and Peles 2003).

Kv channels contain four  $\alpha$  subunits (MacKinnon 1991) and based on homology of the  $\alpha$  subunits, the family of Kv channels can be divided into four main subfamilies (Jan and Jan 1997): Kv1 (Shaker), Kv2 (Shab), Kv3 (Shaw), and Kv4 (Shal). In neurons, the distinct distribution and biophysical properties of Kv channels are also thought to be controlled by combination of subunits.

In myelinated axons, Kv channels containing Kv1.1 subunits are important for axonal conduction at juxtaparanodal regions and axonal terminal of peripheral nervous system (David, Modney et al. 1995; Rasband 2004). They are sensitive to 4-aminopyridine (4-AP) and tetraethylammonium (TEA) and are located in highest concentration in the juxtaparanodal region (Wang, Kunkel et al. 1993), with lower densities present in the internode (Roper and Schwarz 1989). Functionally, Kv1.1 channels are likely to be responsible for limiting the re-excitation of the node of Ranvier following conduction of an action potential (Barrett and Barrett 1982; Waxman and Ritchie 1993; Krishnan, Lin et al. 2009). Kv1.1 channels also contribute to the generation of an internodal resting potential, necessary for the maintenance of a stable nodal resting potential (Chiu and Ritchie 1984; Krishnan, Lin et al. 2009).

During demyelination, exposure of Kv1.1 channels increase, which in turn may lead to a decrease in action potential amplitude and duration, due to clamping of the resting membrane potential close to the  $K^+$  equilibrium potential (Waxman and Ritchie 1993; Krishnan, Lin et al. 2009). Additionally, demyelination leads to a diffusion of Kv1.1 channels into paranodal and internodal regions, due to the loss of structural molecules that normally anchor these channels to the juxtaparanodal region (Boyle, Berglund et al. 2001;

Krishnan, Lin et al. 2009). The abnormalities of ion channel configuration may increase in paranodal capacitance and reduce resistance, with consequent reduction in conduction velocity (Boyle, Berglund et al. 2001; Krishnan, Lin et al. 2009). In animal models of demyelination, administration of 4-AP has therefore been suggested as a possible treatment in demyelinating disorders on account of its role in reversing conduction failure (Sherratt, Bostock et al. 1980; Bostock, Sears et al. 1981; Krishnan, Lin et al. 2009).

Based on above studies, demyelination associated with the distribution of Kv1.1 channel is an important factor contributing to the loss of axonal function. Other studies have also stated that demyelination associated with the distribution of Kv1.1 channel lead to development of significant neurological deficits in many disorders including multiple sclerosis, spinal cord injury, and other types of neurotrauma (Blight and Decrescito 1986; Nashmi and Fehlings 2001; Judge and Bever 2006; Bagchi, Al-Sabi et al. 2014).

In clinic, axonal dysfunction with voltage-gated potassium channels antibodies have been recently identified (Park, Lin et al. 2014). A number of autoimmune conditions have been linked to the production of antibodies targeting voltage-gated potassium channel-complex components, including neuromyotonia, Morvan's syndrome, limbic encephalitis and forms of epilepsy (Newsom-Davis and Mills 1993; Hart, Waters et al. 1997; Vincent, Buckley et al. 2004). Other neuronal channelopathies associated with Kv1.1 channel also lead to neurological disorders. It has been reported that mutations in KCNA1 gene, encoding the fast potassium channel subunit Kv1.1, are associated with episodic ataxia type 1, which is characterized by brief episodes of cerebellar dysfunction lasting seconds to minutes and by persistent neuromyotonia (Browne, Gancher et al. 1994). Patients with episodic ataxia type 1 also have an increased incidence of epilepsy (Zuberi, Eunson et al. 1999). There are other phenotypes, including neuromyotonia only and distal weakness (Eunson, Rea et al. 2000; Klein, Boltshauser et al. 2004; Chen, von Hehn et al. 2007; Demos, Macri et al. 2009). Recently, studies of nerve excitability were performed to characterize Kv1.1 channel dysfunction in patients with episodic ataxia type 1, but the results were not as the authors expected, and consumed more researches to be clarified (Tomlinson, Tan et al. 2010; Park, Lin et al. 2014; Kuwabara and Misawa 2015).

Injured axons can be repaired by end-to-end neurorrhaphy (EEN). However, there are several differences in remyelinated nerve fiber, as compared with axons before injury. Juxtaparanodal Kv channels normally are isolated electrically but are uncovered after demyelination and during nerve regeneration, reducing excitability. Although Na<sup>+</sup> channel distributions subsequent to demyelination have been well known (Bostock and Sears 1978; Shrager 1987) (Dugandzija-Novakovic, Koszowski et al. 1995; Novakovic, Deerinck et al. 1996), much less is known about the relationship between Kv channels and potassium ion

distribution during remyelination. However, traditional potassium indicator assay of cytosolic free  $K^+$  did not successfully evaluate intracellular potassium concentration in the formalin-fixed mammalian tissues. We tried to overcome the problem to obtain  $K^+$  image at regenerating axons by using time-of-flight secondary ion mass spectrometry (TOF-SIMS).

The specific patterns of Kv1.1 channel contribute to axonal conduction velocity during axon regeneration. We hypothesize that change in the quantity of re-arrangement Kv channel could lead to efflux of potassium ion at the juxtaparanodal regions of the remyelinated axon. The goal of this study is to characterize the expression, distribution, and the dynamic changes in Kv1.1 channels of EEN-rat model.

## **Materials and methods**

### ***Experimental animals***

Young adult male Wistar weighing 200-300 g ( $n = 18$ ) were obtained from the Laboratory Animal Center of the Chung Shan Medical University and were used in this study. All experimental animals were housed under the same conditions with controlled temperature and humidity. In the care and handling of all experimental animals, the Guide for the Care and Use of Laboratory Animals (1985) as stated in the United States NIH Guidelines (NIH publication no. 86-23) were followed. All experimental procedures with surgical intervention were approved by the Laboratory Animal Center Authorities of the Chung Shan Medical University (IACUC Approval No 1760).

### ***Surgical procedures***

The in vivo model of PNI were performed by means of end-to-end neurorrhaphy (EEN) as described in our previous studies (Liao, Chen et al. 2009; Liao, Chen et al. 2010; Chang, Shyu et al. 2013). Briefly, after deeply anesthetized with intraperitoneal injection of 7% chloral hydrate (Sigma-Aldrich, St. Louis, MO, USA), rats were placed on the surgical microscope and an incision was made along the left mid-clavicular line to expose the left brachial plexus. The musculocutaneous nerve (McN) was then transected at the margin of the pectoralis major muscle. The end of the proximal ulnar nerve (UN) was then neurorrhaphied to the end of the distal McN (Oberlin, Beal et al. 1994) with 10-0 nylon sutures (Ethilon, Edinburgh, UK) under a surgical microscope. The wound was closed with 5-0 silk and animals were allowed to survive for 1–3 months following surgery. Immediately after EEN, all operated animals were divided into two groups with six in each. Group I (EE1M group) were received end-to-end neurorrhaphy for 30 days, whereas Group II (EE3M group) were received end-to-end neurorrhaphy for 90 days, respectively. Additional six animals without surgical intervention were served as normal control.

### ***Perfusion and tissue preparation***

For TOF-SIMS and immunohistochemical study, at the end of the survival period after EEN, half of the experimental animals from all groups were deeply anesthetized with 7% chloral hydrate (0.4 mL/100g) and were subjected to transcardiac perfusion with 100 mL of Ringer's solution, followed by 45 min of fixation with 4% paraformaldehyde in 0.1 M phosphate buffer (PB), pH=7.4. After perfusion, the distal end of the repaired nerve was removed under a dissecting microscope and kept in a similar fixative for 2 hours. The tissue block was then immersed in graded concentrations of sucrose buffer (10-30%) for cryoprotection at 4°C overnight. Serial 25- $\mu$ m-thick sections of the nerve segment were cut longitudinally with a cryostat (CM3050S, Leica Microsystems, Wetzlar, Germany) on the following day. For immunoblotting, another half of the experimental animals deeply anesthetized were perfused with Ringer's solution and then the musculocutaneous nerves were quickly removed under a dissecting microscope. The samples were stored at -80°C until use.

#### ***Kv channel and PGP 9.5 immunofluorescence stain***

For Kv channels and PGP 9.5 immunohistochemistry, tissue sections collected were first placed in the blocking medium containing 0.1% Triton X-100, 3% normal goat serum and 2% bovine serum albumin (all from Sigma-Aldrich, St. Louis, MO, USA) for 1 hour to block nonspecific binding. After several washes in phosphate buffer saline (PBS), the sections were incubated in rabbit polyclonal anti-Kv1.1 antibody (1:100, Alomone Laboratories, Jerusalem, Israel), and mouse polyclonal PGP 9.5 antibody (1:500, Eugene, OR, USA) with the blocking medium for 24 hours at 4°C. After incubation in primary antibodies, the sections were further incubated with Alexa Fluor anti-mouse IgG (1:200, Jackson Immuno-Research, West Grove, PA, USA), Cy3-conjugated anti-rabbit IgG (1:200, Jackson Immuno-Research, West Grove, PA, USA) and Hoechst 33342 anti-rabbit IgG (1:500, *Dako*, Carpinteria, CA, USA) to visualize PGP 9.5, Kv channels and nuclei, respectively. All mounted sections were examined and photomicrographed under the confocal fluorescence microscope (SP5, Leica Microsystems, Wetzlar, Germany).

#### ***Western blotting***

Musculocutaneous nerve tissue samples were subjected to Western blot analysis. Briefly, the musculocutaneous nerves removed from experimental animals were firstly homogenized with Kaplan buffer (50 mM Tris buffer, pH=7.4, 150 mM NaCl, 10% glycerol, 1% NP40, and protease inhibitor cocktail) and clarified by centrifugation. Following that, equal amounts of solubilized proteins and cell lysates were separated on SDS-PAGE (10%) and electroblotted onto a nitrocellulose membranes (Bio-Rad Laboratories, Hercules, CA, USA). The membranes were then blocked with 5% skim milk and probed with antibodies against  $\beta$ -actin (1:10000, *BD Biosciences*, San Jose, CA, USA),

Kv1.1 channel (1:1000, Alomone Laboratories, Jerusalem, Israel), PGP 9.5 (1:150, BCAM, Cambridge, UK) at 4°C overnight. After incubation with primary antibodies, the membranes were incubated with horseradish peroxidase-conjugated secondary antibodies (Bethyl Laboratories, Montgomery, TX, USA) at a dilution of 1:10000 for 1 hour at room temperature. The immunoreactions were visualized with ECL solution (Millipore, Temecula, CA, USA) followed by 2 minutes of film exposure.

### ***TOF-SIMS analysis***

TOF-SIMS analysis was carried out on a TOF-SIMS IV instrument (ION-TOF GmbH, Münster, Germany). The gallium ( $\text{Ga}^+$ ) ion gun was operated at 25 kV using as the primary ion source (1 pA pulse current) for experiments conducted in this study. The  $\text{Ga}^+$  primary ion beam was scanned over an area of  $100 \mu\text{m}^2$ . Positive secondary ions flying through a reflectron mass spectrometer were detected with a micro-channel plate assembly operating at 10 kV postacceleration. Mass calibration of the ion spectrum was achieved by using a set of mass peaks like  $m/z = 15$  ( $\text{CH}_3^+$ ), 41 ( $\text{C}_3\text{H}_5^+$ ), 69 ( $\text{Ga}^+$ ), and paraformaldehyde molecule since this element was the major component in the tissue matrix following vascular fixation (Chang, Liao et al. 2012). The ions related to  $\text{K}^+$  ( $m/z = 39$ ) were used to identify and evaluate the molecular image of potassium expression.

### ***Statistical Analysis***

For TOF-SIMS analysis, spectral intensity detected from each section was normalized to the ion intensity of paraformaldehyde (serve as base line = 100%) and was expressed as the percentage above the base line (Chang, Liao et al. 2012). All quantitative data acquired from spectrometric, immunofluorescent, and immunoblotting in normal and EEN rats were subjected to one-way ANOVA followed by Bonferroni *post hoc* test. Data were presented as means  $\pm$  SD.  $P < 0.05$  is considered statistically significant.

## Results

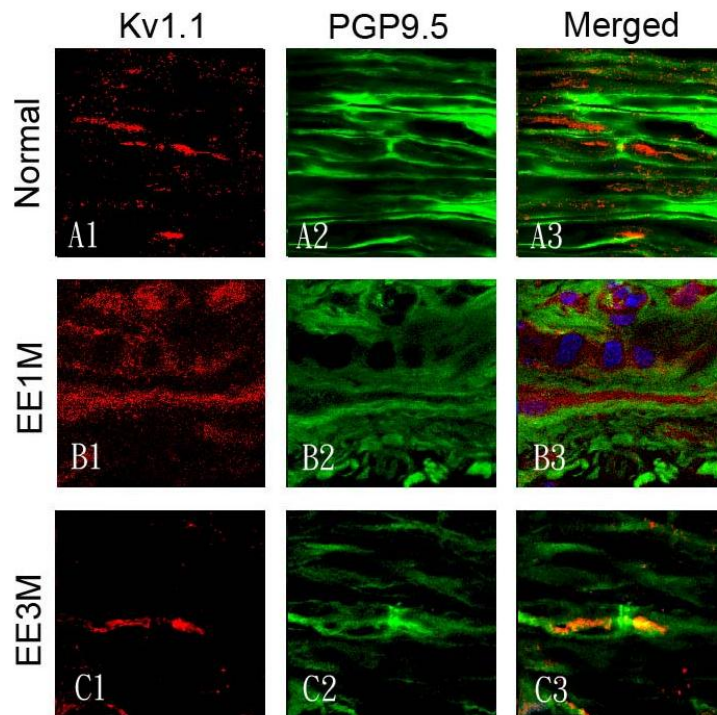


**Fig.1** Confocal photomicrographs showing distribution of Kv1.1 channels and PGP 9.5 at node of Ranvier of regenerating axons. The recipient nerve tissues were immunostained with anti-PGP9.5 antibody (green) and anti-Kv1.1 polyclonal antibody (red) 1 and 3 months following EEN. Representative images are shown. Cell nuclei were counterstained with Hoechst 33342 (blue). The distribution of Kv1.1 channels was concentrated in the juxtapanodal region (Fig. A1 and A3). Whereas, Kv1.1 channels scattered throughout the regenerating nerve fibers 1 month following EEN (Fig. B1 and B3). Note that Kv1.1 channels underwent a structural rearrangement at juxtapanodal region 3 months following EEN (Fig. C1 and C3).

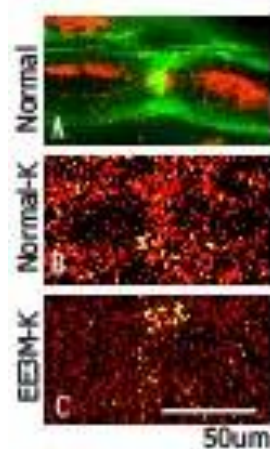


**Fig. 2** Ionic imaging showing the  $K^+$  expression at node of Ranvier of regenerating axons. Confocal image showed that the normal nerve was immunostained with anti-PGP9.5 antibody (green) and anti-Kv1.1 polyclonal antibody (red; Fig. 2A). Ionic image showed



the in vivo K<sup>+</sup> expression and normalized spectral intensity for K<sup>+</sup> in the musculocutaneous nerve of normal and EEN rats. The ionic imaging of K<sup>+</sup> signaling is expressed by a color scale in which bright colors represent high levels of K<sup>+</sup>. Strong K<sup>+</sup> intensities were scattered outside the juxtapanodal region of the musculocutaneous nerve in normal rats (Fig. 2B). Furthermore, most of the K<sup>+</sup> were rearranged and concentrated at the node of Ranvier 3 months following EEN (yellow spots; Fig. 2C). Scale bar = 50 μm.

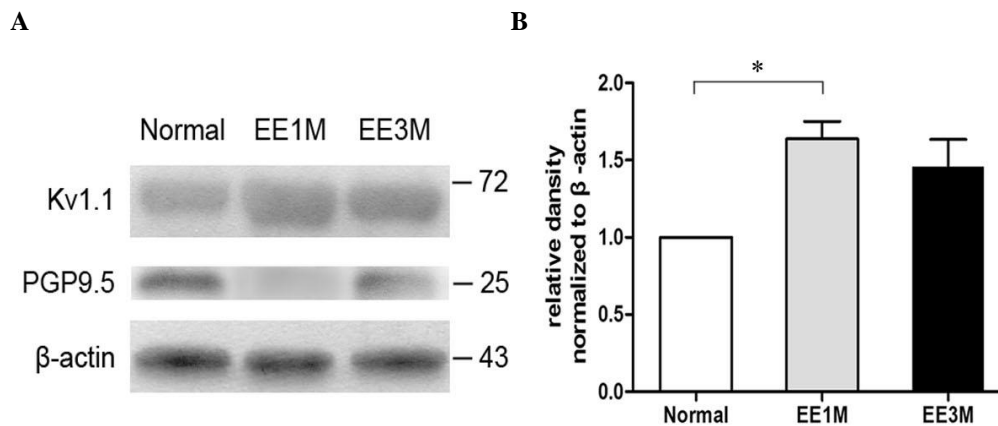


**Fig.3** Immunoblotting (Fig. 3A) and histogram (Fig. 3B) showing Kv1.1 channel expression in nerve tissues of normal and 1-3month EEN rats. Expressions of PGP 9.5 (24 kDa) and Kv1.1 channel (72 kDa) were detected. β-actin is the loading control (Fig. 3A). Densitometric analysis indicated a higher ratio of Kv1.1 channel to β-actin in EE1M groups as compared to that of normal control ones (Fig. 3B). The Kv1.1 channel expression in EE1M group was 1.58-fold higher than in normal control group. Furthermore, EE3M group showed a 1.49-fold increase in the ratio of Kv1.1 channel to β-actin (Fig. 3B). Values are means ± SD. \**P* < 0.05 as compared to that of control value.

## Discussion

The generation of the action potential in nerve requires a complete series of the components between ion channels and ion. Using the novel application of TOF-SIMS, the present study has provided the first functional anatomical evidence to show interaction between the localization of Kv1.1 channel and potassium ionic distribution at juxtapanodal region of the regenerating axons (Fig.1 and Fig.2).

An injury to the peripheral nerve system could cause disorganization of Kv1.1 channel distribution, leading to colocalisation with nodal Na<sup>+</sup> channels and disruption of the paranode in demyelinated axons (Rasband, Trimmer et al. 1998; Arroyo, Xu et al. 1999; Rasband 2004). The increased activity of Kv1.1 channels may reduce membrane excitability, leading to conduction block as the membrane potential approaches the K<sup>+</sup> equilibrium potential (Nashmi and Fehlings 2001). Since Kv1.1 channels shifted to the

node and paranode, impulse conduction has been impaired. Moreover, during nerve remyelination, the transient presence of Kv1.1 channels at the node may act to repolarize the membrane potential and prevent repetitive activity (Rasband, Trimmer et al. 1998).

Kv1.1 channel/PGP9.5 double immunofluorescence was performed in the present study. We reported that Kv1.1 channels located on juxtaparanodal region of the normal myelinated axons and scattered throughout the regenerating axons at the time 1 month following EEN (Fig. 1). At three months following EEN, Kv1.1 channels reorganized to juxtaparanodal region of the regenerating axons. The result suggested that these rearranged Kv1.1 channels may act to modulate the neuronal excitability through stabilizing membrane potential, prevent repetitive discharges during late stage of nerve regeneration.

In addition, we found that efflux of potassium ion was clustered at peri-nodal region of normal nerve tissue with TOF-SIMS. The ionic imaging illustrated that the outflow of potassium ion was decreased and clustered at node of Ranvier of EE3M-rats (Fig. 2). In previous studies, the low potassium expression at juxtaparanodal region was not easy to cause repolarization of the membrane potential (Kuwabara et al., 2002; Krishnan et al., 2005). The low  $K^+$  concentration had also correlated with excitability abnormalities, suggesting that the duration of action potential were prolonged and could not exert normal conduction velocities. Furthermore, the densitometric analysis of immunoblotting showed that scattered Kv1.1 channels was highly expressed in regenerated nerve samples at 1 month, whereas expression of re-concentrated Kv1.1 channels was partially decreased 3 months after EEN (Fig. 3).

We suggest that dynamic changes in the re-arrangement Kv1.1 channel could regulate efflux of potassium ion at juxtaparanodal regions of the regenerating axon, thus contribute to electrical stability of the nodal potential. To selectively trap potassium ions at peri-nodal region may improve the treatment of slow nerve conduction velocity in patients. The obtained information will not only improve our understanding of Kv1.1 channel in the initial stage of nerve regeneration, but also provide insights into Kv channels targeting drugs, for the clinical usage of PNI.

## References

1. Arroyo, E. J., Y. T. Xu, et al. (1999). "Myelinating Schwann cells determine the internodal localization of Kv1.1, Kv1.2, Kvbeta2, and Caspr." *J Neurocytol* **28**(4-5): 333-347.
2. Bagchi, B., A. Al-Sabi, S. Kaza, D. Scholz, V. B. O'Leary, J. O. Dolly and S. V. Ovsepian (2014). "Disruption of Myelin Leads to Ectopic Expression of KV1.1 Channels with Abnormal Conductivity of Optic Nerve Axons in a Cuprizone-Induced Model of Demyelination." *PLoS One* **9**(2): e87736.

3. Barrett, E. F. and J. N. Barrett (1982). "Intracellular recording from vertebrate myelinated axons: mechanism of the depolarizing afterpotential." J Physiol **323**: 117-144.
4. Blight, A. R. and V. Decrescito (1986). "Morphometric analysis of experimental spinal cord injury in the cat: the relation of injury intensity to survival of myelinated axons." Neuroscience **19**(1): 321-341.
5. Bostock, H. and T. A. Sears (1978). "The internodal axon membrane: electrical excitability and continuous conduction in segmental demyelination." J Physiol **280**: 273-301.
6. Bostock, H., T. A. Sears, et al. (1981). "The effects of 4-aminopyridine and tetraethylammonium ions on normal and demyelinated mammalian nerve fibres." J Physiol **313**: 301-315.
7. Boyle, M. E., E. O. Berglund, et al. (2001). "Contactin orchestrates assembly of the septate-like junctions at the paranode in myelinated peripheral nerve." Neuron **30**(2): 385-397.
8. Browne, D. L., S. T. Ganchar, et al. (1994). "Episodic ataxia/myokymia syndrome is associated with point mutations in the human potassium channel gene, KCNA1." Nat Genet **8**(2): 136-140.
9. Chang, H. M., W. C. Liao, et al. (2012). "Sleep deprivation impairs Ca<sup>2+</sup> expression in the hippocampus: ionic imaging analysis for cognitive deficiency with TOF-SIMS." Microsc Microanal **18**(3): 425-435.
10. Chang, H. M., M. K. Shyu, et al. (2013). "Neuregulin facilitates nerve regeneration by speeding Schwann cell migration via ErbB2/3-dependent FAK pathway." PLoS One **8**(1): e53444.
11. Chen, H., C. von Hehn, et al. (2007). "Functional analysis of a novel potassium channel (KCNA1) mutation in hereditary myokymia." Neurogenetics **8**(2): 131-135.
12. Chiu, S. Y. and J. M. Ritchie (1984). "On the physiological role of internodal potassium channels and the security of conduction in myelinated nerve fibres." Proc R Soc Lond B Biol Sci **220**(1221): 415-422.
13. David, G., B. Modney, et al. (1995). "Electrical and morphological factors influencing the depolarizing after-potential in rat and lizard myelinated axons." J Physiol **489** ( Pt 1): 141-157.
14. Demos, M. K., V. Macri, et al. (2009). "A novel KCNA1 mutation associated with global delay and persistent cerebellar dysfunction." Mov Disord **24**(5): 778-782.
15. Eunson, L. H., R. Rea, et al. (2000). "Clinical, genetic, and expression studies of mutations in the potassium channel gene KCNA1 reveal new phenotypic variability."

Ann Neurol **48**(4): 647-656.

16. Evans, G. R. (2001). "Peripheral nerve injury: a review and approach to tissue engineered constructs." Anat Rec **263**(4): 396-404.
17. Hart, I. K., C. Waters, et al. (1997). "Autoantibodies detected to expressed K<sup>+</sup> channels are implicated in neuromyotonia." Ann Neurol **41**(2): 238-246.
18. Jan, L. Y. and Y. N. Jan (1997). "Cloned potassium channels from eukaryotes and prokaryotes." Annu Rev Neurosci **20**: 91-123.
19. Judge, S. I. and C. T. Bever, Jr. (2006). "Potassium channel blockers in multiple sclerosis: neuronal Kv channels and effects of symptomatic treatment." Pharmacol Ther **111**(1): 224-259.
20. Klein, A., E. Boltshauser, et al. (2004). "Episodic ataxia type 1 with distal weakness: a novel manifestation of a potassium channelopathy." Neuropediatrics **35**(2): 147-149.
21. Krishnan, A. V., C. S. Lin, et al. (2009). "Axonal ion channels from bench to bedside: a translational neuroscience perspective." Prog Neurobiol **89**(3): 288-313.
22. Kuwabara, S. and S. Misawa (2015). "Acquired and genetic channelopathies: in vivo assessment of axonal excitability." Exp Neurol **263**: 368-371.
23. Liao, W. C., J. R. Chen, et al. (2009). "The efficacy of end-to-end and end-to-side nerve repair (neurorrhaphy) in the rat brachial plexus." J Anat **215**(5): 506-521.
24. Liao, W. C., J. R. Chen, et al. (2010). "Methylcobalamin, but not methylprednisolone or pleiotrophin, accelerates the recovery of rat biceps after ulnar to musculocutaneous nerve transfer." Neuroscience **171**(3): 934-949.
25. MacKinnon, R. (1991). "Determination of the subunit stoichiometry of a voltage-activated potassium channel." Nature **350**(6315): 232-235.
26. Nashmi, R. and M. G. Fehlings (2001). "Mechanisms of axonal dysfunction after spinal cord injury: with an emphasis on the role of voltage-gated potassium channels." Brain Res Brain Res Rev **38**(1-2): 165-191.
27. Newsom-Davis, J. and K. R. Mills (1993). "Immunological associations of acquired neuromyotonia (Isaacs' syndrome). Report of five cases and literature review." Brain **116** ( Pt 2): 453-469.
28. Oberlin, C., D. Beal, et al. (1994). "Nerve transfer to biceps muscle using a part of ulnar nerve for C5-C6 avulsion of the brachial plexus: anatomical study and report of four cases." J Hand Surg Am **19**(2): 232-237.
29. Park, S. B., C. S. Lin, et al. (2014). "Axonal dysfunction with voltage gated potassium channel complex antibodies." Exp Neurol **261**: 337-342.
30. Poliak, S. and E. Peles (2003). "The local differentiation of myelinated axons at nodes of Ranvier." Nat Rev Neurosci **4**(12): 968-980.

31. Priestley, J. V. (2007). "Promoting anatomical plasticity and recovery of function after traumatic injury to the central or peripheral nervous system." Brain **130**(Pt 4): 895-897.
32. Rasband, M. N., J. S. Trimmer, et al. (1998). "Potassium channel distribution, clustering, and function in remyelinating rat axons." J Neurosci **18**(1): 36-47.
33. Rasband, M. N. (2004). "It's "juxta" potassium channel!" J Neurosci Res **76**(6): 749-757.
34. Roper, J. and J. R. Schwarz (1989). "Heterogeneous distribution of fast and slow potassium channels in myelinated rat nerve fibres." J Physiol **416**: 93-110.
35. Sherratt, R. M., H. Bostock, et al. (1980). "Effects of 4-aminopyridine on normal and demyelinated mammalian nerve fibres." Nature **283**(5747): 570-572.
36. Shrager, P. (1987). "The distribution of sodium and potassium channels in single demyelinated axons of the frog." J Physiol **392**: 587-602.
37. Tomlinson, S. E., S. V. Tan, et al. (2010). "Nerve excitability studies characterize Kv1.1 fast potassium channel dysfunction in patients with episodic ataxia type 1." Brain **133**(Pt 12): 3530-3540.
38. Vincent, A., C. Buckley, et al. (2004). "Potassium channel antibody-associated encephalopathy: a potentially immunotherapy-responsive form of limbic encephalitis." Brain **127**(Pt 3): 701-712.
39. Wang, H., D. D. Kunkel, et al. (1993). "Heteromultimeric K<sup>+</sup> channels in terminal and juxtaparanodal regions of neurons." Nature **365**(6441): 75-79.
40. Waxman, S. G. and J. M. Ritchie (1993). "Molecular dissection of the myelinated axon." Ann Neurol **33**(2): 121-136.
41. Zuberi, S. M., L. H. Eunson, et al. (1999). "A novel mutation in the human voltage-gated potassium channel gene (Kv1.1) associates with episodic ataxia type 1 and sometimes with partial epilepsy." Brain **122** ( Pt 5): 817-825.
42. Krishnan, A.V., Colebatch, J.G., Kiernan, M.C. (2005). "Hypokalemic weakness in hyperaldosteronism: activity-dependent conduction block." Neurology **65**(8): 1309-1312.
43. Kuwabara, S., Kanai, K., Sung, J.Y., Ogawara, K., Hattori, T., Burke, D., Bostock, H.(2002). "Axonal hyperpolarization associated with acute hypokalemia: multiple excitability measurements as indicators of the membrane potential of human axons." Muscle Nerve **26**(2): 283-287.